Inorg. Chem. **2005**, *44*, 8762–8769

Non-Interpenetrated Square-Grid Coordination Polymers Synthesized Using an Extremely Long *N*,*N*′-Type Ligand

Chun-Long Chen,[†,‡] Andrea M. Goforth,[†] Mark D. Smith,[†] Cheng-Yong Su,[‡] and Hans-Conrad zur Loye*[,†]

Department of Chemistry and Biochemistry, University of South Carolina, Columbia, South Carolina 29208, and School of Chemistry and Chemical Engineering, Sun Yat-Sen University, Guangzhou 510275, China

Received June 28, 2005

Four new, non-interpenetrated square-grid coordination polymers, namely $[Mn(L)_2(NO_3)_2]_\infty$ (**1**), $\{[Cd(L)_2(NO_3)_2]\cdot solvate\}_\infty$ (**2**), $[Cd(L)_2(NO_3)_2]_\infty$ (**3**), and $\{[Zn(L)_2](BF_4)_2\cdot(C_6H_6)_{2.564}\cdot(DMF)_{1.576}\cdot(MeOH, H_2O)_{3.454}\}_\infty$ (**4**), were synthesized using the new, extremely long *N*,*N*′-type ligand: 2,5-bis(4′-(imidazol-1-yl)benzyl)-3,4-diaza-2,4-hexadiene (L). The reaction of $Cd(NO_3)_2$ with L leads to two novel structures sharing the same framework composition, $[Cd(L)_2(NO_3)_2]_\infty$, which have different arrangements of L around the metal centers. Both the channel-containing structure and the nonporous structure can be formed by choice of the appropriate solvent system. Moreover, the less stable, channel-containing form readily converts into the more stable, condensed structure upon removal of the guest molecules from the channels.

Introduction

The synthesis and investigation of new coordination polymers is of current interest in the fields of supramolecular chemistry and crystal engineering not only because of their intrinsic aesthetic appeal but also because of their potential for utilization in a variety of applications.[1] Due to rapid advances during the past several years, the field of supramolecular chemistry is progressing to the point where desired supramolecular structures can often be synthesized via self-assembly of judiciously selected building blocks under controlled reaction conditions. One aspect, in particular, that has greatly affected the field of supramolecular chemistry is the design and synthesis of new ligands, which continues to play an important role in the formation of new supramolecular complexes with desired structures and concomitant properties.[2]

Among the numerous coordination polymer structures that have been documented, the square-grid topology stands out as an important network class because of the desirable applications associated with such networks (e.g., in heterogeneous catalysis[3]) and also because the formation of this structure type is often highly predictable. It is well-known that long, rodlike *N*,*N*′-type ligands can lead to square-grid structures containing large cavities when they are reacted with metals capable of adopting (pseudo) octahedral or (pseudo) square planar coordination geometries.[4] Furthermore, it is generally accepted that longer ligands often favor the formation of interpenetrating square-grid structures.[4e,5] However, interpenetration can often be reduced, or even avoided completely, by identifying and controlling certain reaction conditions (e.g., solvent system and reagent concentration).

We have been exploring the synthesis of new coordination polymers based on rigid *N*,*N*′-type ligands,[4d,5b,6] including

* To whom correspondence should be addressed. E-mail: zurloye@mail.chem.sc.edu.
† University of South Carolina.
‡ Sun Yat-Sen University.

(1) (a) Dro, C.; Bellemin-Laponnaz, S.; Welter, R.; Gade, L. H. *Angew. Chem., Int. Ed.* **2004**, *43*, 4479. (b) Yoshizawa, M.; Miyagi, S.; Kawano, M.; Ishiguro, K.; Fujita, M. *J. Am. Chem. Soc.* **2004**, *126*, 9172. (c) Chun, H.; Dybtsev, D. N.; Kim, H.; Kim, K. *Chem.—Eur. J.* **2005**, *11*, 3521 and references therein. (d) Su, C.-Y.; Cai, Y.-P.; Chen, C.-L.; Lissner, F.; Kang, B.-S.; Kaim, W. *Angew. Chem., Int. Ed.* **2002**, *41*, 3371. (e) Su, C.-Y.; Cai, Y.-P.; Chen, C.-L.; Smith, M. D.; Kaim, W.; zur Loye, H.-C. *J. Am. Chem. Soc.* **2003**, *125*, 8595.
(2) Steel, P. J. *Acc. Chem. Res.* **2005**, *38*, 243 and references therein.
(3) Ohmori, O.; Fujita, M. *Chem. Commun.* **2004**, 1586.
(4) (a) Biradha, K.; Hongo, Y.; Fujita, M. *Angew. Chem., Int. Ed.* **2000**, *39*, 3843. (b) Ohmori, O.; Kawano, M.; Fujita, M. *CrystEngComm* **2004**, *6* (11), 51. (c) Takaoka, K.; Kawano, M.; Tominaga, M.; Fujita, M. *Angew. Chem., Int. Ed.* **2005**, *44*, 2151. (d) Pschirer, N. G.; Ciurtin, D. M.; Smith, M. D.; Bunz, U. H. F.; zur Loye, H.-C. *Angew. Chem., Int. Ed.* **2002**, *41*, 583. (e) Dong, Y.-B.; Wang, P.; Huang, R.-Q.; Smith, M. D. *Inorg. Chem.* **2004**, *43*, 4727.
(5) (a) Halder, G. J.; Kepert, C. J.; Moubaraki, B.; Murray, K, S.; Cashion, J. D. *Science* **2002**, *298*, 1762. (b) Su, C.-Y.; Goforth, A. M.; Smith, M. D.; zur Loye, H.-C. *Chem. Commun.* **2004**, 2158. (c) Biradha, K.; Fujita, M. *Chem. Commun.* **2002**, 1866.

10.1021/ic051068o CCC: $30.25
Published on Web 10/18/2005

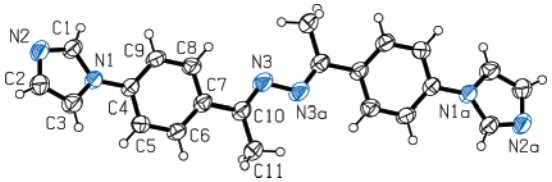

Figure 1. Molecular structure and atom labeling scheme for the new ligand 2,5-bis(4′-(imidazol-1-yl)benzyl)-3,4-diaza-2,4-hexadiene (L). Thermal ellipsoids are drawn at the 50% probability level.

the following: 1,4-bis(4-pyridyl)butadiyne,[6a] 1,4-bis(3-pyridyl)-2,3-diaza-1,3-butadiene,[6b] 1,4-bis(4-pyridyl)-2,3-diaza-1,3-butadiene,[6b] 9,9-diethyl-2,7-bis(4-pyridylethynyl)fluorene, and 9,9-bis[(*S*)-2-methylbutyl]-2,7-bis(4-pyridylethynyl)-fluorene.[4d] In all these examples, the specific geometries of these ligands have allowed us to obtain numerous coordination polymers with interesting structures. To further study coordination polymers based on *N*,*N*′-type ligands and to target the preparation of large, non-interpenetrated square-grid coordination polymers, we synthesized the new, extremely long ligand 2,5-bis(4′-(imidazol-1-yl)benzyl)-3,4-diaza-2,4-hexadiene (L) (Figure 1). Using this ligand, we achieved the synthesis of four new, non-interpenetrated square-grid coordination polymers, including two Cd-containing structures sharing the same framework composition, $[Cd(L)_2(NO_3)_2]_\infty$. Interestingly, the solvent of crystallization influences the formation of the specific structure formed, and conversion of the less stable, channel-containing structure to the more stable, condensed structure occurs as a solid-to-solid transformation. Dynamic behavior in coordination polymers has been observed previously;[7] nonetheless, the transformation of an open framework into a condensed structure via solvent loss, as described herein, is rather unusual.

Experimental Section

Materials and Methods. All starting materials and solvents were obtained from commercial sources and were used without further purification. IR spectra in the 4000−400 cm^{-1} region were recorded on a Shimadzu FTIR-8400 spectrophotometer using KBr as reference. ^1H NMR spectra were collected at room temperature on a Varian Mercury/VX 300 spectrometer with chemical shifts reported in δ relative to DMSO-d_6. X-ray powder diffraction (XRD) patterns were acquired on a Rigaku D\Max-2200 powder X-ray diffractometer with graphite monochromatized Cu Kα radiation (λ = 0.15418 nm). Thermogravimetric analyses (TGAs) were carried out on a TA Instruments SDT 2960 simultaneous DTA-TGA under flowing helium by heating the compounds from 25 to 1000 °C using a heating rate of 10 °C/min.

Synthesis. (A) Preparation of the Ligand (L). Hydrazine (35% solution in water, 0.46 g) was added dropwise to a stirred solution of 4-(imidazol-1-yl)acetophenone in methanol (20 mL). Then, after the addition of four drops of glacial acetic acid, the mixture was refluxed for 3 h and subsequently cooled to room temperature. A yellow precipitate was obtained, and after recrystallization from hot methanol, the yellow crystalline product was harvested in 72% yield. ^1H NMR (DMSO-d_6, ppm): 8.37 (t, 2H, H1), 8.06 (m, 4H, H4), 7.85 (t, 2H, H2), 7.77 (m, 4H, H5), 7.15 (t, 2H, H3), 2.34 (s, 6H, H6). IR (KBr, cm^{-1}): 3112 (m), 3074 (w), 3047 (w), 3020 (w), 2978 (w), 1605 (s), 1570 (m), 1520 (s), 1481 (m), 1420 (m), 1369 (s), 1323 (w), 1304 (s), 1261 (w), 1188 (m), 1111 (m), 1057 (s), 1030 (w), 1011 (w), 980 (w), 961 (m), 903 (w), 864 (w), 829 (s), 764 (w), 745 (m), 660 (s), 621 (w), 567 (m), 536 (m), 505 (m). Elemental analysis (%) calcd for $C_{22}H_{20}N_6$: C, 71.72; H, 5.47; N, 22.81. Found: C, 71.50; H, 5.63; N, 22.76.

(B) Preparation of the Complexes. (a) $[Mn(L)_2(NO_3)_2]_\infty$ (1). $Mn(NO_3)_2 \cdot 6H_2O$ (0.05 mmol) dissolved in MeOH (3 mL) was layered onto a solution of L (0.05 mmol) in DMSO (3 mL). After 1 week, yellow plate crystals suitable for X-ray analysis had formed at the bottom of the test tube. Yield: 65%. IR (KBr, cm^{-1}): 3132 (m), 3071 (w), 3047 (w), 2916 (w), 1620 (m), 1605 (s), 1578 (w), 1524 (s), 1489 (m), 1420 (m), 1412 (m), 1366 (m), 1323 (s), 1304 (s), 1269 (w), 1250 (m), 1188 (m), 1123 (m), 1061 (s), 1015 (w), 964 (m), 930 (m), 837 (s), 756 (m), 756 (m), 670 (m), 625 (w), 571 (m), 517(w). Elemental analysis (%) calcd for $MnC_{44}H_{40}N_{14}O_6$: C, 57.71; H, 4.40; N, 21.41. Found: C, 57.70; H, 4.47; N, 21.11.

(b) $\{[Cd(L)_2(NO_3)_2]\cdot solvate\}_\infty$ (2) and $[Cd(L)_2(NO_3)_2]_\infty$ (3). $Cd(NO_3)_2 \cdot 4H_2O$ (0.05 mmol) dissolved in MeOH (3 mL) was layered onto a solution of L (0.05 mmol) in DMF and benzene (1:1, 3 mL). Crystals started to form during the second day at the interface between the DMF/benzene and MeOH layers. After one week, yellow plate crystals (**2**) and yellow block crystals (**3**) suitable for single-crystal X-ray diffraction analysis could be harvested. Crystals of **2** are extremely unstable in air, and upon removal from the mother liquor, they lose guest solvent molecules and quickly transform into polycrystalline **3**. ^1H NMR (DMSO-d_6, ppm): 8.38 (2H, H1), 8.06 (4H, H4), 7.86 (2H, H2), 7.78 (4H, H5), 7.17 (2H, H3), 2.34 (s, 6H, H6). IR (KBr, cm^{-1}): 3132 (m), 3071 (w), 3047 (w), 2916 (w), 1620 (m), 1605 (s), 1558 (w), 1524 (s), 1489 (m), 1420 (m), 1404 (m), 1366 (m), 1327 (s), 1308 (s), 1269 (w), 1250 (m), 1188 (m), 1126 (m), 1061 (s), 1015 (w), 964 (m), 930 (m), 837 (s), 756 (m), 656 (s), 625 (w), 567 (m), 513(w). Elemental analysis (%) calcd for $CdC_{44}H_{40}N_{14}O_6$ (desolvated **2** and **3**): C, 54.30; H, 4.14; N, 20.15. Found for a mixture of compounds **2** and **3** after mild heating: C, 52.45; H, 4.15; N, 19.24.

(c) $[Cd(L)_2(NO_3)_2]_\infty$ (3). $Cd(NO_3)_2 \cdot 4H_2O$ (0.05 mmol) dissolved in MeOH (3 mL) was layered onto a solution of L (0.05 mmol) in DMSO (3 mL). After one week, yellow block-shaped crystals suitable for single-crystal X-ray diffraction analysis had formed at the bottom of the vial. The yield of phase-pure crystals of **3** was 60%.

(6) (a) Zaman, M. B.; Smith, M. D.; zur Loye, H.-C. *Chem. Mater.* **2001**, *13*, 3534. (b) Dong, Y.-B.; Smith, M. D.; zur Loye, H.-C. *Inorg. Chem.* **2000**, *39*, 4927. (c) Ciurtin, D. M.; Dong, Y.-B.; Smith, M. D.; Barclay, T.; zur Loye, H.-C. *Inorg. Chem.* **2001**, *40*, 2825. (d) Zaman, M. B.; Smith, M. D.; Ciurtin, D. M.; zur Loye, H.-C. *Inorg. Chem.* **2002**, *41*, 4895.

(7) Kitagawa, S.; Uemura, K. *Chem. Soc. Rev.* **2005**, *34*, 109. Matsuda, R.; Kitaura, R.; Kitagawa, S.; Kubota, Y.; Kobayashi, T. C.; Horike, S.; Takata, M. *J. Am. Chem. Soc.* **2004**, *126*, 14063. Choi, H. J.; Suh, M. P. *J. Am. Chem. Soc.* **2004**, *126*, 15844. Barea, E.; Navarro, J. A. R.; Salas, J. M.; Masciocchi, N.; Galli, S.; Sironi, A. *J. Am. Chem. Soc.* **2004**, *126*, 3014. Kondo, M.; Irie, Y.; Shimizu, Y.; Miyazawa, M.; Kawaguchi, H.; Nakamura, A.; Naito, T.; Maeda, K.; Uchida, F. *Inorg. Chem.* **2004**, *43*, 6139. Biradha, K.; Hongo, Y.; Fujita, M. *Angew. Chem., Int. Ed.* **2002**, *41*, 3395. Wu, C.-D.; Lin, W. *Angew. Chem., Int. Ed.* **2005**, *44*, 1958. Saied, O.; Maris, T.; Wuest, J. D. *J. Am. Chem. Soc.* **2003**, *125*, 14956. Dybtsev, D. N.; Chun, H.; Kim, K. *Angew. Chem., Int. Ed.* **2004**, *43*, 5033. Choi, E.-Y.; Park, K.; Yang, C.-M.; Kim, H.; Son, J.-H.; Lee, S. W.; Lee, Y. H.; Min, D.; Kwon, Y.-U. *Chem.—Eur. J.* **2004**, *10*, 5535. Halder, G. J.; Kepert, C. J. *J. Am. Chem. Soc.* **2005**, *127*, 7891. Zhao, X. B.; Xiao, B.; Fletcher, A. J.; Thomas, K. M.; Bradshaw, D.; Rosseinsky, M. J. *Science* **2004**, *306*, 1012. Lee, E. Y.; Jang, S. Y.; Suh, M. P. *J. Am. Chem. Soc.* **2005**, *127*, 6374. Lee, I. S.; Shin, D. M.; Chung, Y. K. *Chem.—Eur. J.* **2004**, *10*, 3158.

Table 1. Crystallographic Data for L and **1**−**4**

	L	**1**	**2**	**3**	**4**
empirical formula	$C_{22}H_{20}N_6$	$C_{44}H_{40}MnN_{14}O_6$	$C_{44}H_{40}CdN_{14}O_6$	$C_{44}H_{40}CdN_{14}O_6$	$C_{66.64}H_{66.41}B_2F_8N_{13.57}O_{5.03}Zn$
formula weight	368.44	915.84	973.30	973.30	1377.00
crystal system	monoclinic	monoclinic	triclinic	monoclinic	monoclinic
space group	$P2_1/n$	$P2_1/c$	$P\bar{1}$	$P2_1/c$	$P2_1/n$
a (Å)	8.4037(5)	8.5036(5)	10.1647(7)	8.5646(5)	10.2553(7)
b (Å)	7.4235(4)	23.8157(13)	20.6265(13)	23.7881(13)	19.4349(14)
c (Å)	14.9619(9)	10.2711(6)	22.0519(15)	10.3148(6)	37.201(3)
α (deg)	90	90	63.1510(10)	90	90
β (deg)	94.2840(10)	90.6880(10)	86.9200(10)	90.7960(10)	91.131(3)
γ (deg)	90	90	82.8230(10)	90	90
V (Å^3)	930.79(9)	2079.9(2)	4092.7(5)	2101.3(2)	7413.1(9)
Z	2	2	3	2	4
ρ_{calc} (g/cm^3)	1.315	1.462	1.185	1.538	1.234
μ(Mo Kα) (mm^{-1})	0.082	0.387	0.453	0.588	0.406
temperature (K)	294(1)	150(1)	150(1)	150(1)	150(1)
R1[a]	0.0394	0.0489	0.0540	0.0344	0.0724
wR2[b]	0.1098	0.1237	0.1214	0.0835	0.1865

(d) Procedure for the Solid-State Transformation of 2 into 3. Freshly prepared plate-shaped crystals of **2**, chosen based on crystal habit, were removed from the mother liquor, and a powder X-ray diffraction pattern was immediately acquired. Following the X-ray experiment, the sample was heated to 150 °C for 2 h, and upon cooling the sample, a second diffraction pattern was acquired. The pattern of the sample following heat treatment is the same as that calculated from the single-crystal diffraction data for compound **3**.

(e) $\{[Zn(L)_2](BF_4)_2\cdot(C_6H_6)_{2.564}\cdot(DMF)_{1.576}\cdot(MeOH, H_2O)_{3.454}\}_\infty$ (4). $Zn(BF_4)_2\cdot 6H_2O$ (0.05 mmol) dissolved in MeOH (3 mL) was layered onto a solution of L (0.05 mmol) in DMF and benzene (1:1, 3 mL). Crystals started to form during the second day at the interface between the DMF/benzene and MeOH layers. After one week, yellow plate crystals suitable for X-ray analysis could be harvested. Yield: 62%. IR (KBr, cm^{-1}): 3144 (m), 3067 (w), 1605 (m), 1528 (s), 1423 (w), 1365 (m), 1334 (m), 1308 (m), 1261 (m), 1250 (m), 1188 (w), 1126 (m), 1084 (s), 1069 (s), 1038 (m), 1015 (m), 968 (m), 887 (w), 841 (m), 745 (w), 656 (m), 621 (w). Elemental analysis (%) calcd for $ZnC_{44}H_{40}N_{12}B_2F_8$ (desolvated **4**): C, 54.16; H, 4.13; N, 17.22. Found for **4** after heating to 200 °C to remove solvent molecules: C, 54.28; H, 4.46; N, 16.98.

Crystallography. X-ray intensity data from an irregular yellow crystal cleaved from a larger sample were measured at 294(1) K (L) or 150(1) K (**1**−**4**) on a Bruker SMART APEX CCD-based diffractometer (Mo Kα radiation, $\lambda = 0.71073$ Å).[8] Raw data frame integration and Lp corrections were performed with SAINT+.[8] Final unit cell parameters were determined by the least-squares refinement of 4999 (L), 7678 (**1**), 6507 (**2**), 6407 (**3**), and 6891 (**4**) reflections from the respective data sets with $I > 5\sigma(I)$. Analysis of the data in all cases showed negligible crystal decay during collection. Direct methods structure solution, difference Fourier calculations, and full-matrix least-squares refinement against F^2 were performed with SHELXTL.[9] Non-hydrogen atoms were refined with anisotropic displacement parameters. Hydrogen atoms were placed in geometrically idealized positions and included as riding atoms. A summary of the crystal data is given in Table 1. Selected interatomic distances are listed in Table 2. Selected bond angles are available in the Supporting Information. The data collection and structure solutions of **2** and **4** are noteworthy, and a detailed description of these experiments is available in the Supporting Information.

(8) Sheldrick, G. M. *SHELXTL*, version 6.1; Bruker Analytical X-ray Systems, Inc.: Madison, WI, 2000.

(9) *SMART*, version 5.625; Bruker Analytical X-ray Systems, Inc.: Madison, WI, 2001. *SAINT+*, version 6.22; Bruker Analytical X-ray Systems, Inc.: Madison, WI, 2001.

Table 2. Selected Interatomic Distances (Å) for Complexes **1**−**4**

	Complex **1**[a]		
Mn(1)−O(1)$^{\#1}$	2.211(2)	Mn(1)−N(6)$^{\#3}$	2.224(2)
Mn(1)−O(1)	2.211(2)	Mn(1)−N(1)$^{\#1}$	2.274(2)
Mn(1)−N(6)$^{\#2}$	2.224(2)	Mn(1)−N(1)	2.274(2)
	Complex **2**[b]		
Cd(1)−N(12)$^{\#1}$	2.290(3)	Cd(2)−N(16A)	2.266(4)
Cd(1)−N(7)	2.312(3)	Cd(2)−N(16B)$^{\#5}$	2.266(4)
Cd(1)−N(1)	2.325(3)	Cd(2)−N(16A)$^{\#5}$	2.266(4)
Cd(1)−O(1)	2.336(4)	Cd(2)−N(13)$^{\#5}$	2.357(4)
Cd(1)−N(6)$^{\#2}$	2.338(4)	Cd(2)−N(13)	2.357(4)
Cd(1)−O(4)	2.410(3)	Cd(2)−O(7)	2.426(4)
Cd(2)−O(7)	2.426(4)	Cd(2)−O(7)$^{\#5}$	2.426(4)
		Cd(2)−O(7)$^{\#5}$	2.426(4)
	Complex **3**[c]		
Cd(1)−N(6)$^{\#1}$	2.2913(16)	Cd(1)−N(1)$^{\#3}$	2.3537(15)
Cd(1)−N(6)$^{\#2}$	2.2913(16)	Cd(1)−O(1)	2.3721(17)
Cd(1)−N(1)	2.3537(15)	Cd(1)−O(1)$^{\#3}$	2.3721(17)
	Complex **4**[d]		
Zn(1)−N(7)$^{\#1}$	1.986(4)	Zn(1)−N(12)	2.008(4)
Zn(1)−N(6)$^{\#2}$	1.988(4)	Zn(1)−N(1)	2.013(4)

[a] Symmetry code: (#1) $-x, -y, -z+1$; (#2) $x-2, -y+1/2, z+1/2$; (#3) $-x+2, y-1/2, -z+1/2$. [b] Symmetry code: (#1) $x+1, y-1, z$; (#2) $x, y, z+1$; (#3) $x, y, z-1$; (#4) $x-1, y+1, z$; (#5) $-x+1, -y+1, -z+1$. [c] Symmetry code: (#1) $x-2, -y+1/2, z+1/2$; (#2) $-x+2, y-1/2, -z+1/2$; (#3) $-x, -y, -z+1$. [d] Symmetry code: (#1) $-x-1/2, y+1/2, -z+1/2$; (#2) $x-1/2, -y+1/2, z-1/2$.

Results and Discussion

Synthesis and Crystal Structure of the Ligand (L). The new ligand, 2,5-bis(4′-(imidazol-1-yl)benzyl)-3,4-diaza-2,4-hexadiene (L), was readily prepared in 72% yield by the condensation of hydrazine hydrate with 4-(imidazol-1-yl)-acetophenone. Due to the large size of its terminal group, the present ligand (L) is significantly longer than other known hydrazine-based ligands.[6b,6c] Furthermore, because of the possibility of free rotation around the Ar−C single bonds, this ligand is considerably more flexible than other *N*,*N*′-type Schiff-base ligands that we have previously synthesized.[6b,6c] Four possible configurations (hereafter referred to as I, II, III, or IV) that may be adopted by L are shown in Scheme 1.

Crystals of L were obtained by allowing a methanol solution of L to evaporate slowly. The structure of L was confirmed by single-crystal X-ray diffraction, which established that the ligand adopts the *transoid* configuration (I**)** in the solid state. While the ligand is nonplanar overall, the

Scheme 1 Four Possible Configurations of the Ligand L

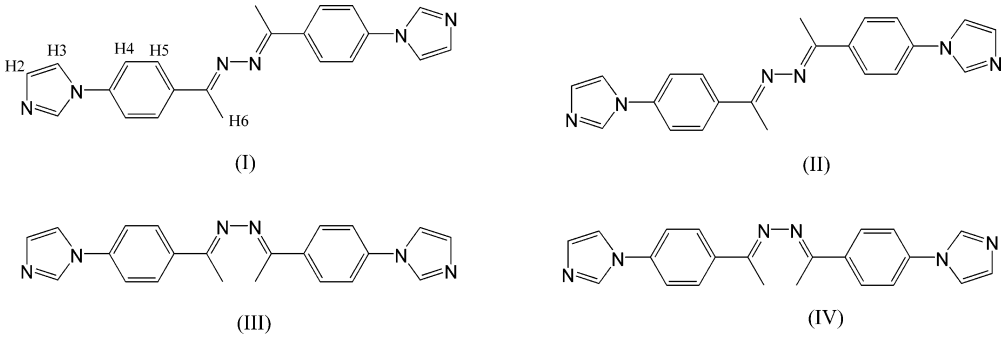

central phenylimine fragment (the ligand minus the two imidazol-1-yl groups) is planar and the dihedral angle between the imidazol-1-yl group and the phenyl group is 31.95(7)°. The terminal imidazolyl N···N separation in L is rather long at 18.174(5) Å, and it is significantly longer than the terminal N···N separations found in most other *N*,*N*′-type rigid ligands reported to date.[4e,6] The long length of L, together with its terminal N-donor sites, is expected to enable the formation of large square grid coordination polymers. Reactions between the ligand and various metal salts were accomplished by allowing the slow interdiffusion of two solutions containing the components. It is worthwhile to mention that, in the reaction between L and $Cd(NO_3)_2$, the solvent system was found to significantly affect the formation of the final compound(s). In this case, a two phase product mixture was obtained from the initial solvent system, and subsequent adjustment of the exact solvent composition was employed to obtain product **3** as a phase-pure solid.

Crystal Structures of the Complexes. Complex **1** was obtained as yellow plate crystals by layering $Mn(NO_3)_2 \cdot 6H_2O$ in MeOH onto L in DMSO. Single-crystal analysis revealed that **1** crystallizes in the monoclinic crystal system in the $P2_1/c$ space group. The asymmetric unit contains one ligand, one monodentate NO_3^- anion, and half of a Mn(II) atom. The manganese atom is located on an inversion center and adopts an octahedral coordination environment consisting of four N-donors (Mn(1)−N(6)#2 = 2.224(2) Å, Mn(1)−N(6)-#3 = 2.224(2) Å, Mn(1)−N(1)#1 = 2.274(2) Å, and Mn(1)−N(1) = 2.274(2) Å) from four crystallographically equivalent L ligands and two O-donors (Mn(1)−O(1)#1 = 2.211(2) Å and Mn(1)−O(1) = 2.211(2) Å) from two crystallographically equivalent NO_3^- anions (Figure 2).

In this complex, L adopts configuration II (Scheme 1) and acts as a bridge between two Mn(II) atoms in such a way that it generates a "buckled" two-dimensional (2D) layer in the *ab* plane. Alternatively, the layered arrangement may be viewed as an array of intersecting right- and left-handed helical chains ($[MnL]_n$) running along the crystallographic *b*-direction, as shown in Figure 3. The right- and left-handed helical chains intersect via common Mn(II) atoms, resulting in two-dimensional sheets having a (4,4) topology in the *ab* plane. The size of the M_4L_4 square is about 2.1 × 2.1 nm^2 (calculated using the positions of the Mn(II) atoms), which is larger than the size of the square grids observed in many related complexes generated from *N*,*N*′-type rigid ligands.[3,4a,4c,4e,6a,6c] Surprisingly, the layers are non-interpenetrated despite the large cavity size. However, the ABCD-ABCD stacking of the square-grid layers prevents substantial void space in the structure. As shown in Figure 4, the four offset, consecutive nets obstruct any potential channel and, consequently, no guest solvent molecules can be found in this non-interpenetrated structure.

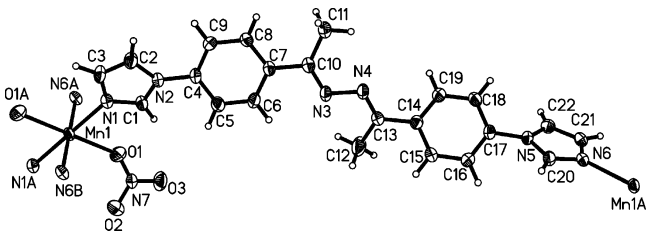

Figure 2. Thermal ellipsoid plot (50% probability) and atom labeling scheme for complex **1**, $[Mn(L)_2(NO_3)_2]_\infty$.

When L is reacted with $Cd(NO_3)_2$ in a DMF/benzene/MeOH solvent environment, both complex **2** and complex **3** form in the same reaction mixture. Interestingly, single-crystal analysis revealed that **2** and **3** share the same framework composition, $[Cd(L)_2(NO_3)_2]_\infty$, although **2** contains solvents of crystallization and **3** is a condensed structure. In addition, complex **3** is isostructural with complex **1**.

Complex **2** crystallizes in the triclinic system with the space group $P\bar{1}$. The structure is affected by the extensive disorder of both the host framework and the guest solvent

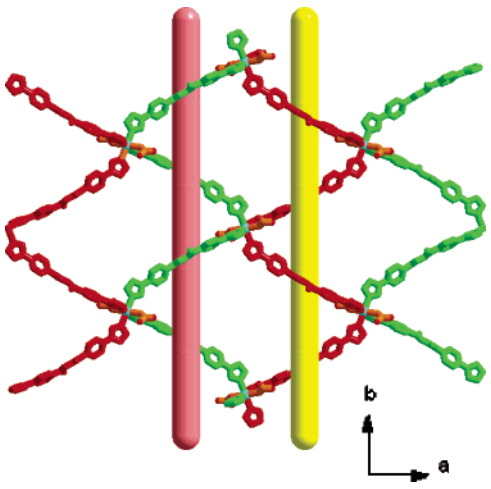

Figure 3. Schematic of the square grid structure of **1**, $[Mn(L)_2(NO_3)_2]_\infty$, and of the isostructural **3**, $[Cd(L)_2(NO_3)_2]_\infty$, emphasizing the right- or left-handed (green and red, respectively) helical chains.

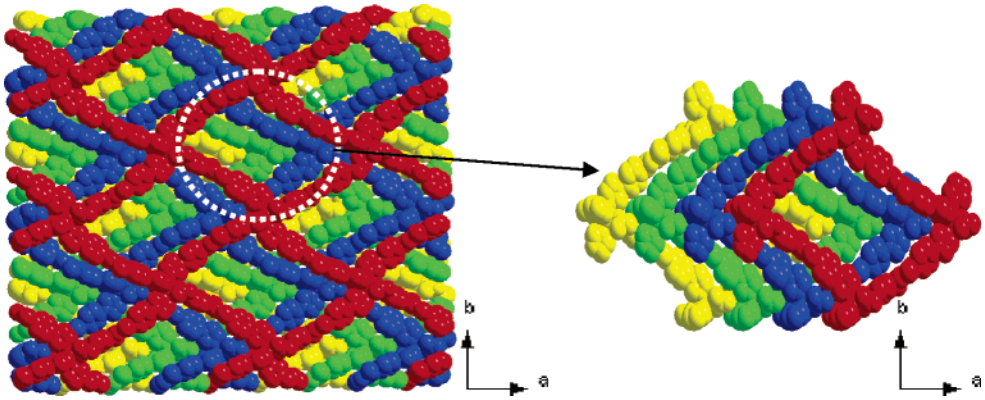

Figure 4. Schematic of the ABCDABCD stacking of the square-grid layers of **1**, $[Mn(L)_2(NO_3)_2]_\infty$, and of the isostructural **3**, $[Cd(L)_2(NO_3)_2]_\infty$. To aid the viewer, each grid is shown in a different color.

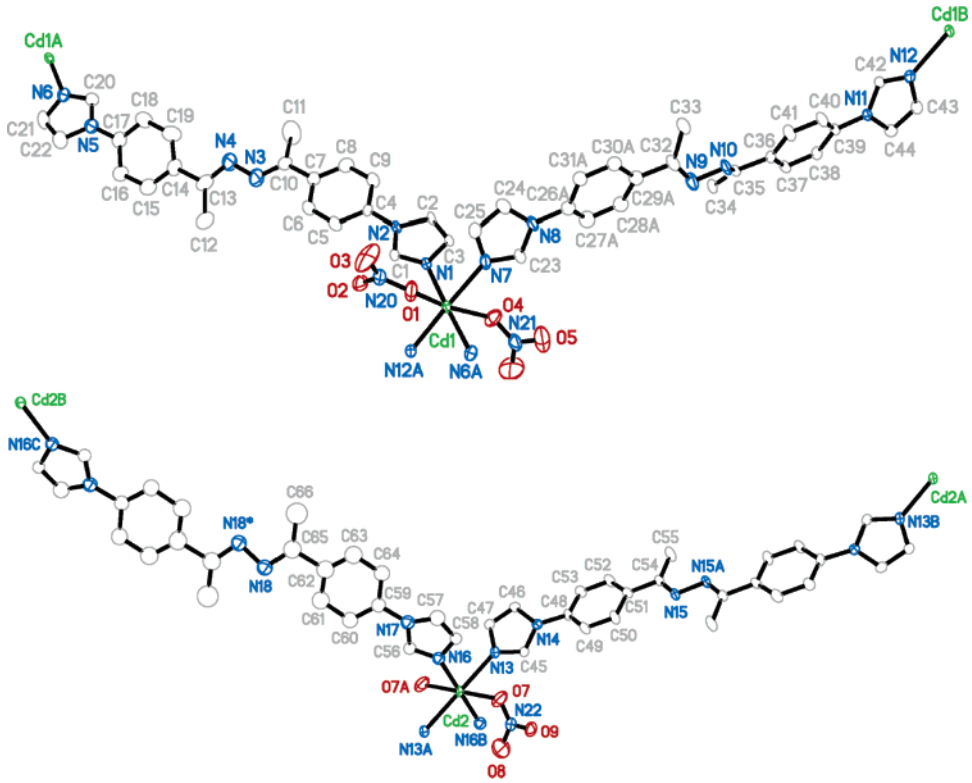

Figure 5. Thermal ellipsoid plots (50% probability) and atom labeling schemes for the two independent nets containing Cd1 (top) and Cd2 (bottom) in complex **2**, $\{[Cd(L)_2(NO_3)_2]\cdot solvate\}_\infty$.

molecules. In complex **2**, there are 1.5 crystallographically independent $[Cd(L)_2(NO_3)_2]$ moieties, which contain two crystallographically distinct Cd centers, Cd1 and Cd2. As shown in Figure 5, Cd1 and Cd2 both adopt octahedral coordination environments, and each is coordinated to four N-donors from L ligands and two O-donors from nitrate groups. Each crystallographically distinct cadmium is involved in the formation of a unique square-grid layer. The dimensions of the square grids in the two layers are both ca. 2.2×2.2 nm^2 (calculated using the positions of the Cd(II) atoms). Again, surprisingly, the layers are non-interpenetrated, despite their large cavity size. In contrast to the crystal packing in the isostructural compounds **1** and **3**, the ABCABC stacking of the square grids found in **2** creates infinite channels along the *b*-axis (Figure 6). The solvent-accessible volume of these channels, calculated with the PLATON program,[10] is 1089.4 Å^3 or 26.6% of the total unit cell volume. These channels are occupied by many disordered solvent molecules, which could not be crystallographically identified or well refined. A view parallel to the stacking direction of the square-grid layers shows that they are essentially planar and that the ligands adopt configuration I, rather than the configuration observed in structures **1** and **3** (II).

Due to its channel-containing structure, complex **2** readily loses guest solvent molecules upon removal of the crystals from the mother liquor. Thus, complex **2** is unstable in air, and the absence of the guest molecules triggers a structural

(10) Spek, A. L. *PLATON, A Multipurpose Crystallographic Tool*; Utrecht University: Utrecht, The Netherlands, 1998.

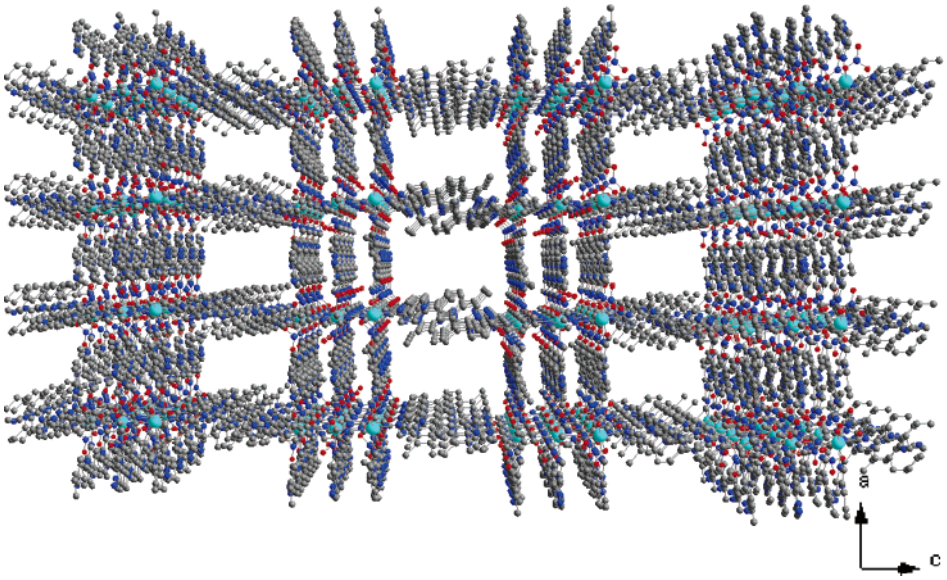

Figure 6. Framework structure of complex **2**, $\{[Cd(L)_2(NO_3)_2]\cdot solvate\}_\infty$. The guest solvent molecules are omitted for clarity.

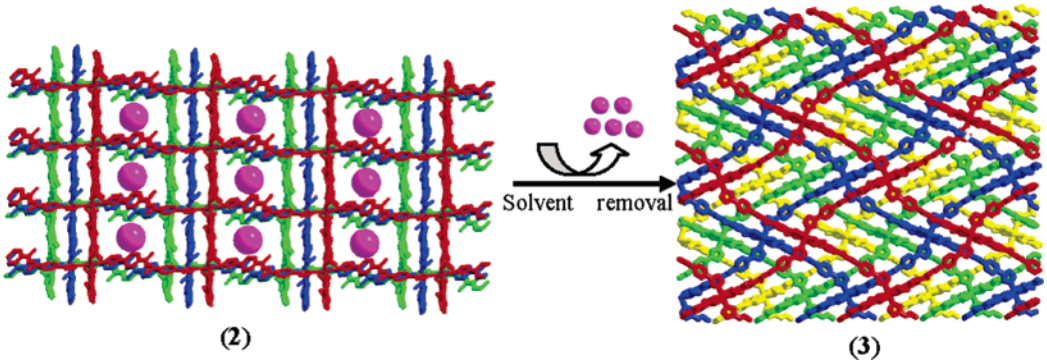

Figure 7. Depiction of the solid-to-solid transformation of complex **2** into complex **3**.

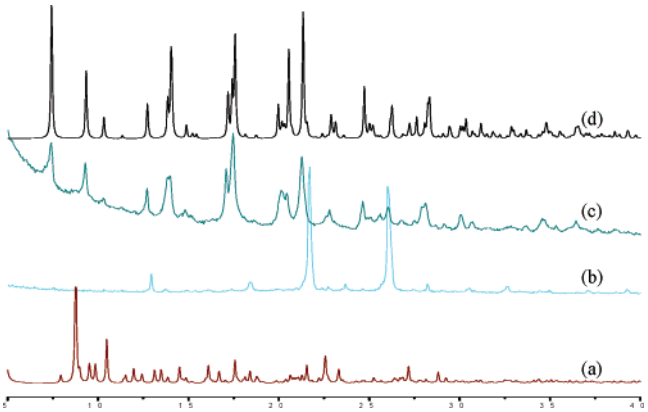

Figure 8. XRD patterns: (a) simulated for **2**; (b) measured for **2** immediately after removal from the mother liquor; (c) measured for **2** after heating to 150°C for 2 h; (d) simulated for **3**.

transformation from structure **2** to structure **3** (Figure 7), as evidenced by the powder X-ray diffraction experiments (Figure 8).

Yellow plate crystals of **4** were obtained from the reaction of L with $Zn(BF_4)_2\cdot 6H_2O$ in a DMF/benzene/MeOH mixed solvent system. The yellow plate crystals of **4** are extremely unstable once removed from the mother liquor, and they must be frozen quickly in order to prevent crystal decomposition prior to the structural analysis. Single-crystal measurement

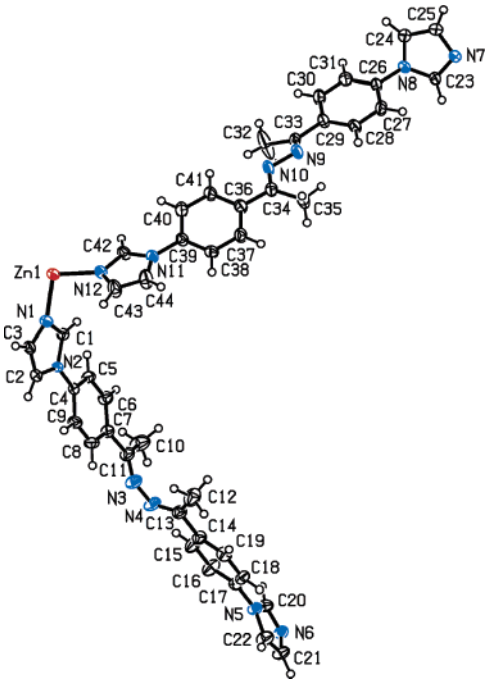

Figure 9. Thermal ellipsoid plot (50% probability) of the asymmetric unit of complex **4** with the atom labeling scheme.

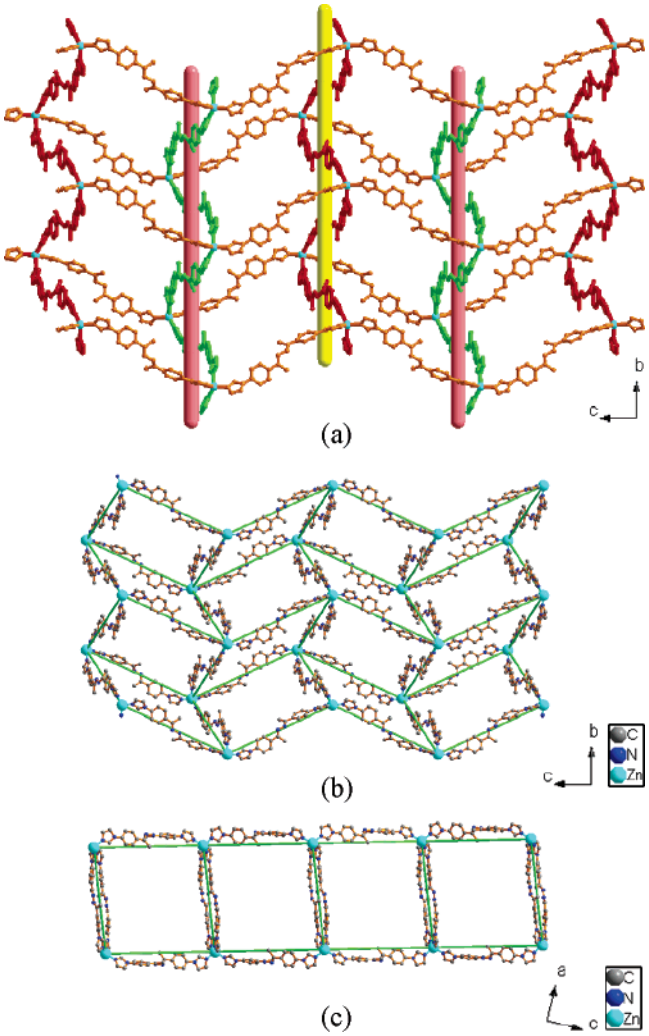

Figure 10. (a) Schematic of the square-grid structure of **4**, $\{[Zn(L)_2](BF_4)_2 \cdot (C_6H_6)_{2.564} \cdot (DMF)_{1.576} \cdot (MeOH, H_2O)_{3.454}\}_\infty$, emphasizing the right- or left-handed (green and red, respectively) helical chains. (b) [010] view of a single 2D sheet having a (4,4) topology. (c) Perpendicular view of b, emphasizing the 1D ladder-type appearance.

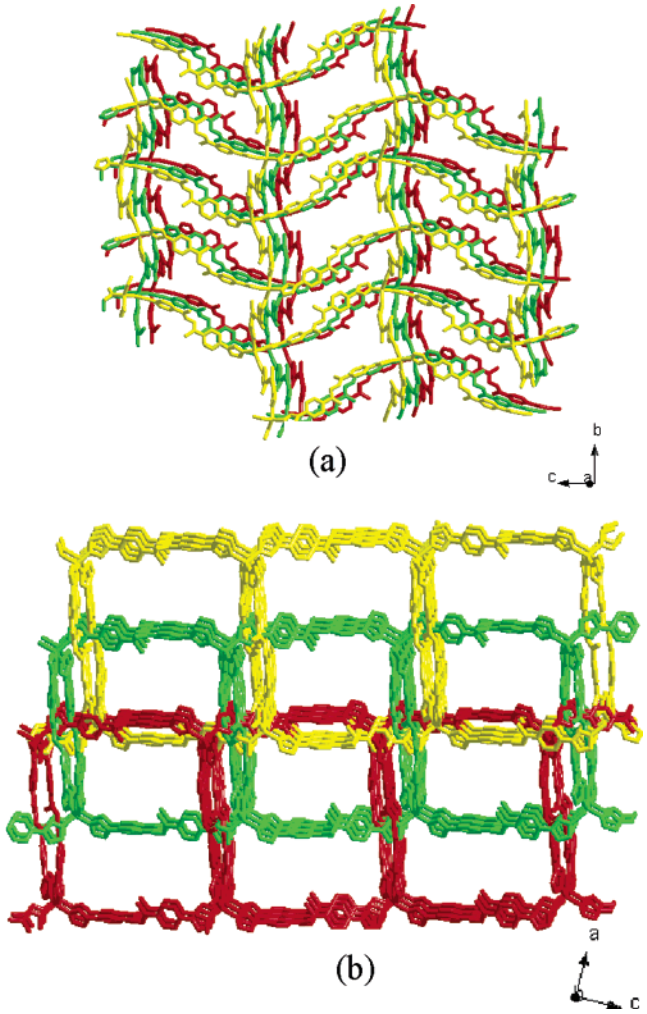

Figure 11. Depiction of the stacking of three square-grid layers in complex **4**, $\{[Zn(L)_2](BF_4)_2 \cdot (C_6H_6)_{2.564} \cdot (DMF)_{1.576} \cdot (MeOH, H_2O)_{3.454}\}_\infty$, that reduces the accessible channel size.

shows that the non-solvent content of the asymmetric unit consists of one Zn atom, two independent L ligands, and two independent noncoordinated BF_4^- anions. The Zn(II) cation is located in a distorted tetrahedral coordination sphere consisting of four N-donors (Zn(1)−N(7)#1 = 1.986(4) Å, Zn(1)−N(6)#2 = 1.988(4) Å, Zn(1)−N(12) = 2.008(4) Å, and Zn(1)−N(1) = 2.013(4) Å) from four L ligands (Figure 9). Half of the μ_2-L ligands connect adjacent zinc centers into right- and left-handed helical chains ($[ZnL]_n$) running in the *b*-axis direction, as shown in Figure 10a. The remaining μ_2-L ligands connect adjacent helical chains to form infinite two-dimensional sheets having a (4,4) topology in the *ac* plane (Figure 10b). The dimensions of each grid are about 2.1 × 2.1 nm^2. Compared to the layers found in complexes **1**, **2**, and **3**, the layers in **4** are severely distorted and very nonplanar. In fact, when viewed from the side, the (4,4) topological layer is reminiscent of a one-dimensional (1D) ladder. Consequently, when the structure is viewed along [010], two different 1D channels are observed (Figure 10c): one channel is formed by the chiral helical chains, while the second one is created by the M_4L_4 grids. Similar to the situation observed in complexes **2** and **3**, the stacking of the square grid layers significantly reduces the accessible channel dimensions (Figure 11).

Thermal Stability and Structural Transformation in the Solid State. Compounds **1** and **3** are isostructural and do not contain any guest solvent molecules. Thus, the collection of powder X-ray diffraction patterns is routine (Figure S1), and it is possible to compare the measured pattern to that calculated from single-crystal data. This is not the case for compounds **2** and **4**, which contain guest molecules and decompose before a powder X-ray diffraction measurement can be made. For both **1** and **3**, the measured patterns are in good agreement with the calculated patterns, indicating that phase-pure samples of **1** and **3** have been prepared. TGA studies on **1** indicate that it is stable up to 310 °C (Figure S2), at which point framework decomposition takes place.

Though it was not possible to directly measure the powder diffraction pattern of **2**, the solid-to-solid transformation of **2** into **3** can be monitored by powder X-ray diffraction. A phase-pure sample of **2** was gathered by harvesting single crystals from the mother liquor (selected based on crystal habit), and a powder X-ray diffraction pattern was im-

mediately acquired (Figure 8b). The measured pattern at this point does not resemble the calculated pattern for **2** or the calculated pattern for **3**, and it is indicative of an initial loss of sample crystallinity upon removal of the crystals from the mother liquor. When the same sample is briefly heated to 150 °C to remove any remaining solvent molecules, the result is transformation of the poorly crystalline powder to crystalline compound **3**, as evidenced by the powder pattern acquired following the heat treatment. Following heating, the measured pattern is the same as that calculated for **3** from the single-crystal data (Figure 8). Notably, the transformation from **2** to **3** can also be accomplished without supplying heat, but on a slower time scale.

Conclusions

The new *N*,*N*′-type ligand 2,5-bis(4′-(imidazol-1-yl)benzyl)-3,4-diaza-2,4-hexadiene has been synthesized and structurally characterized. Its coordination chemistry with several metal salts was investigated, and four non-interpenetrated square-grid coordination polymers were successfully prepared. The complexes all exhibit a non-interpenetrated square-grid type structure, where the stacking of the grids in the structure determines the existence and size of any channels. Due to the presence of the four Ar−C single bonds and the N−N single bond in the ligand, it exhibits significant configurational flexibility that enables it to connect metals into channel-containing and condensed 2D structures. Interestingly, the less stable channel-containing structure can convert to the more stable, solvent free structure.

Acknowledgment. We are grateful for financial support from the National Science Foundation through Grant No. CHE:0314164 and the NNSF of China (No. 20303027).

Supporting Information Available: CIF files, details on the structure solution of **2** and **4**, tables of selected interatomic distances and angles for **1**−**4**, XRD patterns for complexes **1** and **3**, and TGA data. This material is available free of charge via the Internet at http://pubs.acs.org. Also, CCDC-276289-276293 contains the crystallographic data for this paper. These data can be obtained free of charge at www.ccdc.cam.ac.uk/conts/retrieving.html [or from the Cambridge Crystallographic Data Centre (CCDC), 12 Union Road, Cambridge CB2 1EZ, U.K. Fax: +44(0)1223-336033. E-mail: deposit@ccdc.cam.ac.uk.].

IC051068O